

Weak Decay of Λ in Nuclei : Quarks vs Mesons

Kenji Sasaki, Takashi Inoue, and Makoto Oka
*Department of Physics, Tokyo Institute of Technology,
 Meguro, Tokyo 152-8551 Japan.*

Abstract

Decays of Λ in nuclei, nonmesonic mode, are studied by using the $\Lambda N \rightarrow NN$ weak transition potential derived from the meson exchange mechanism and the direct quark mechanism. The decay rates are calculated both for the Λ in symmetric nuclear matter and light hypernuclei. We consider the exchange of six mesons ($\pi, K, \eta, \rho, \omega, K^*$). The form factor in the meson exchange mechanism and short range correlation are carefully studied.

1 Introduction

The Λ particle is a neutral baryon with spin $1/2$ and strangeness -1 . It is unstable and has a finite lifetime of about 263[ps]. The main decay modes of a free Λ particle are the pionic ones,

$$\begin{aligned}\Lambda &\rightarrow p + \pi^- \\ &\rightarrow n + \pi^0\end{aligned}$$

where the final state nucleon has the momentum of about 100[MeV/c]. This is one of the $\Delta S = 1$ non-leptonic weak interaction. The important feature of this free Λ decay is the empirical $\Delta I = 1/2$ rule. The experimental branching ratio of two charge modes, $(\Gamma_{\pi^-}/\Gamma_{\pi^0})_{EXP} \simeq 1.78$, is close to the theoretical one with the assumption of $\Delta I = 1/2$ dominance, $(\Gamma_{\pi^-}/\Gamma_{\pi^0})_{Theory}^{\Delta I=1/2} = 2$. This fact tells us that the decay is dominated by $\Delta I = 1/2$ transition. This $\Delta I = 1/2$ dominance is a prominent feature of all the observed $\Delta S = 1$ non-leptonic weak interactions. However, in the standard theory of electro-weak interaction, there are both $\Delta I = 1/2$ and $\Delta I = 3/2$ components. Thus the effect of strong interaction should be significant for the explanation of enhancement of the $\Delta I = 1/2$ contribution [1].

The nucleus with the Λ hyperon is called Λ hypernucleus, and is expressed ${}^A_\Lambda Z$ where Z is the number of proton and A is the mass number. The Λ hyperon in a nucleus falls into the ground state due to absence of the Pauli blocking effect and, therefore, is regarded as a probe of nuclear interior. Since Λ is not a stable particle, hypernucleus also decays via weak interaction,

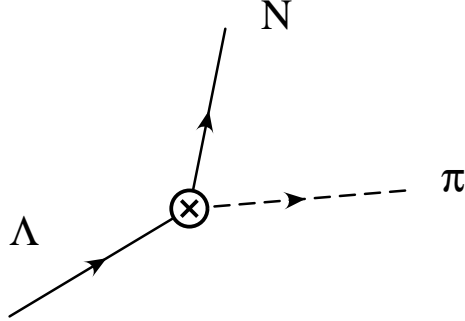


Figure 1: Non-leptonic decay of hyperon.

which is so called weak decay of hypernucleus. It is known that, when the Λ hyperon is in the nuclear medium, the pionic decay mode is strongly suppressed and instead the nucleon induced decay modes,

$$\Lambda + p \rightarrow n + p \quad : \quad \text{proton induced decay} \quad (1)$$

$$\Lambda + n \rightarrow n + n \quad : \quad \text{neutron induced decay} \quad (2)$$

become dominant. This can be understood by considering the Pauli principle for final state nucleons as for the mesonic decay the momentum of the nucleon is less than the Fermi momentum in nuclear matter. In the induced decay mode the momentum of the outgoing nucleons is about $400[\text{MeV}/c]$ (assuming that the relative momentum of the initial Λ and N is zero). It is much larger than the Fermi momentum, $k_F \simeq 270[\text{MeV}/c]$.

The $\Lambda N \rightarrow NN$ transition is the $\Delta S = 1$ reaction analogous to the weak NN interaction or the parity violating part of NN force. Although the weak NN interaction is masked by the overwhelming strong interaction, the $\Lambda N \rightarrow NN$ transition is induced purely by the weak interaction, and therefore it gives us a unique chance to study the mechanism of baryon-baryon weak interaction. At present, the direct observation of the $\Lambda N \rightarrow NN$ process is almost impossible because of the lack of hyperon beam or target. Thus the weak decay of Λ hypernucleus will be one of the clue of research for the $\Lambda N \rightarrow NN$ reaction. Many theoretical and experimental efforts have been devoted to the nonmesonic decays of light and heavy hypernuclei [2-20]. The mechanism of nonmesonic weak decay is still not clear, especially the theoretical prediction of the n/p ratio, which is the ratio of the neutron-induced decay to the proton-induced one, is not compatible with the experimental one. This is because the theoretical value of proton-induced rate is much larger than the experimental one, which is measured to a good precision. The value of the n/p ratio will be a key to understand the mechanism of the nonmesonic decay.

A conventional picture of the two-baryon decay process, $\Lambda N \rightarrow NN$, is the one-pion ex-

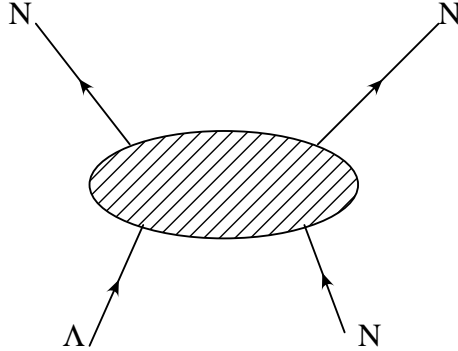


Figure 2: $\Lambda N \rightarrow NN$ transition.

change between the baryons, where $\Lambda N\pi$ vertex is induced by the weak interaction [2, 5, 6, 7]. In $\Lambda N \rightarrow NN$, the relative momentum of the final state nucleon is about 400 MeV/c. The nucleon-nucleon interaction at this momentum is dominated by the short-range repulsion due to heavy meson exchanges and/or to quark exchanges between the nucleons. It is therefore expected that the short-distance interactions will contribute to the two-body weak decay as well. Exchanges of K , ρ , ω , K^* mesons and also correlated two pions in the nonmesonic weak decays of hypernuclei have been studied [3, 4, 8, 9, 10, 15, 16] and it is found that the kaon exchange is significant, while the other mesons contribute less [10].

Several studies have been made on effects of quark substructure [11, 12, 13, 14]. In our recent analysis [13, 14], we employ an effective weak Hamiltonian for quarks. It was pointed out that the $\Delta I = 1/2$ part of the Hamiltonian is enhanced during downscaling of the renormalization point in the renormalization group equation. Yet a sizable $\Delta I = 3/2$ component remains in the low energy effective weak Hamiltonian. We proposed to evaluate the effective Hamiltonian in the six-quark wave functions of the two baryon systems and derived the “direct quark” weak transition potential for $\Lambda N \rightarrow NN$ [13, 14]. Our analysis shows that the direct quark contribution largely improves the discrepancy between the meson-exchange theory and experimental data for the n/p ratios for light hypernuclei. It is also found that the $\Delta I = 3/2$ component of the effective Hamiltonian gives a sizable contribution to $J = 0$ transition amplitudes [12]. Unfortunately, we cannot determine the $\Delta I = 3/2$ amplitudes unambiguously from the present experimental data [17-20].

The aim of this paper is to combine the long-range meson exchange interactions and the short-range direct quark transitions coherently in the study of Λ decay in nuclear matter and in light hypernuclei. We first consider π and K exchanges and further introduce heavier mesons. The direct quark mechanism represents the short-range part of the transition and may therefore

replace the heavy meson exchanges. We compare the results of light + heavy meson exchanges with the results with light mesons + direct quark. For the meson exchange, we particularly study effects of the form factors on the transition rates. The pion exchange amplitudes are found to be sensitive to the choice of the form factors. We propose to use a soft pion-baryon form factors so that the strong tensor transition is suppressed. The direct quark mechanism yields a large neutron-induced amplitude and therefore improves the n/p ratio. We, however, find that its enhancement is not large enough to explain the observed large n/p ratio.

This paper is organized as follows. In section 2, we present the transition potential for the $\Lambda N \rightarrow NN$ transition. In section 3 and 4, the transition potential is applied to the decay in the nuclear matter and light hypernuclei, respectively. Discussions and conclusion are given in section 5.

2 Theoretical approach to $\Lambda N \rightarrow NN$

Since the $\Lambda N \rightarrow NN$ transition involves a large energy transfer, the short range reactions may contribute significantly. Thus we expect that the substructure of the baryons, or the quark degree of freedom play important roles in this transition [11, 12, 13, 14]. In this paper we assume the hybrid mechanism to describe $\Lambda N \rightarrow NN$ decay, meson exchange mechanism (ME) and direct quark mechanism (DQ). Such combination has been successfully employed in describing the strong baryon-baryon interactions.

2.1 Meson Exchange Mechanism

The one pion exchange (OPE) process, where the emitted virtual pion from weak $\Lambda \rightarrow N\pi$ vertex is absorbed by nucleon in the nucleus, shown in Fig. 3, is studied to describe $\Lambda N \rightarrow NN$ decay [2, 5, 6, 7]. This mechanism provides the simplest but indispensable picture because it is based on the main decay mode of the free Λ . This mechanism yields a long range transition potential, which is obtained by evaluating the diagram using the following vertices,

$$\mathcal{H}_s^\pi = ig_{NN\pi} \bar{\psi}_N \gamma_5 \vec{\tau} \cdot \vec{\phi}_\pi \psi_N \quad (3)$$

$$\mathcal{H}_w^\pi = iG_F m_\pi^2 \bar{\psi}_N (A_\pi + B_\pi \gamma_5) \vec{\tau} \cdot \vec{\phi}_\pi \psi_\Lambda. \quad (4)$$

Both the strong coupling constant, $g_{NN\pi}$, and the weak ones, A_π and B_π , are well determined from experiment. Their values are listed in Table 1. It is known that the OPE transition potential enhances the $J = 1$ transition due to the strong tensor term and therefore the amplitude of proton-induced mode is much larger than neutron-induced one. This tensor dominance causes

the n/p ratio problem, namely, the observed n/p ratio ($\simeq 1$) can not be explained by the OPE transition.

While the OPE is significant for the long-distance baryon-baryon interaction, the short range reaction mechanism is also important in $\Lambda N \rightarrow NN$ due to the large energy transfer involved. Within the meson exchange model, a shorter range contributions may come from the exchange of the heavier mesons [3, 4, 8, 9, 10] and correlated two pions meson [15, 16]. In ref [10] the authors consider the exchange of all the octet pseudoscalar and vector mesons, π , K , η , ρ , ω , and K^* . Although the $\Lambda N\pi$ weak coupling constant is determined phenomenologically, all the other weak couplings in ref [10] are estimated theoretically by assuming the $SU(6)_w$ symmetry [9]. While for the strong vertices, the couplings are taken from the Nijmegen YN potential model (soft core) [21].

The strong vertices are given by

$$\mathcal{H}_s^K = ig_{\Lambda NK} \bar{\psi}_N \gamma_5 \phi_K \psi_\Lambda \quad (5)$$

$$\mathcal{H}_s^\eta = ig_{NN\eta} \bar{\psi}_N \gamma_5 \phi_\eta \psi_N \quad (6)$$

$$\mathcal{H}_s^\rho = \bar{\psi}_N \left(g_{NN\rho}^V \gamma^\mu + i \frac{g_{NN\rho}^T}{2M} \sigma^{\mu\nu} q_\nu \right) \vec{\tau} \cdot \vec{\phi}_\mu^\rho \psi_N \quad (7)$$

$$\mathcal{H}_s^{K^*} = \bar{\psi}_N \left(g_{\Lambda NK^*}^V \gamma^\mu + i \frac{g_{\Lambda NK^*}^T}{2M} \sigma^{\mu\nu} q_\nu \right) \phi_\mu^{K^*} \psi_\Lambda \quad (8)$$

$$\mathcal{H}_s^\omega = \bar{\psi}_N \left(g_{NN\omega}^V \gamma^\mu + i \frac{g_{NN\omega}^T}{2M} \sigma^{\mu\nu} q_\nu \right) \phi_\mu^\omega \psi_N \quad (9)$$

while the weak vertices are parameterized as

$$\mathcal{H}_w^K = iG_F m_\pi^2 \left[(\bar{\psi}_N)_s (C_K^{PV} + C_K^{PC} \gamma_5) \phi_K^\dagger \psi_N + \bar{\psi}_N (D_K^{PC} + D_K^{PV} \gamma_5) \psi_N (\phi_K^\dagger)_s \right] \quad (10)$$

$$\mathcal{H}_w^\eta = iG_F m_\pi^2 \bar{\psi}_N (A_\eta + B_\eta \gamma_5) \phi_\eta \psi_\Lambda \quad (11)$$

$$\mathcal{H}_w^\rho = G_F m_\pi^2 \bar{\psi}_N \left(\alpha_\rho \gamma^\mu - \beta_\rho i \frac{\sigma^{\mu\nu} q_\nu}{2M} + \epsilon_\rho \gamma^\mu \gamma_5 \right) \vec{\tau} \cdot \vec{\psi}_\mu^\rho \psi_\Lambda \quad (12)$$

$$\begin{aligned} \mathcal{H}_w^{K^*} = G_F m_\pi^2 & \left([C_{K^*}^{PC,V} (\bar{\psi}_N)_s \phi_\mu^{K^*\dagger} \gamma^\mu \psi_N + D_{K^*}^{PC,V} \bar{\psi}_N \gamma^\mu \psi_N (\phi_\mu^{K^*\dagger})_s] \right. \\ & - i [C_{K^*}^{PC,V} (\bar{\psi}_N)_s K_\mu^{*\dagger} \frac{\sigma^{\mu\nu} q_\nu}{2M} N + D_{K^*}^{PC,V} \bar{\psi}_N \frac{\sigma^{\mu\nu} q_\nu}{2M} \psi_N (\phi_\mu^{K^*\dagger})_s] \\ & \left. + [C_{K^*}^{PV} (\bar{\psi}_N)_s \phi_\mu^{K^*\dagger} \gamma^\mu \gamma_5 \psi_N + D_{K^*}^{PV} \bar{\psi}_N \gamma^\mu \gamma_5 \psi_N (\phi_\mu^{K^*\dagger})_s] \right) \end{aligned} \quad (13)$$

$$\mathcal{H}_w^\omega = G_F m_\pi^2 \bar{\psi}_N \left(\alpha_\omega \gamma^\mu - \beta_\omega i \frac{\sigma^{\mu\nu} q_\nu}{2M} + \epsilon_\omega \gamma^\mu \gamma_5 \right) \phi_\mu^\omega \psi_\Lambda. \quad (14)$$

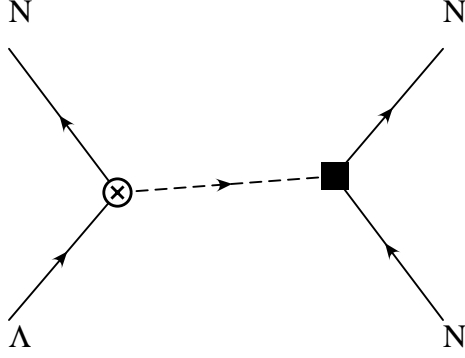


Figure 3: Meson exchange diagram for $\Lambda N \rightarrow NN$ decay. \otimes denotes the weak vertex for the nonstrange mesons and the strong vertex for the strange mesons.

We choose a convention that the three-momentum transfer \mathbf{q} is directed towards to the strong vertex, and we assign the spurious isospin state to the Λ field which behaves like an isospin $|\frac{1}{2} - \frac{1}{2}\rangle$. (The same isospurion $\binom{0}{1}$ is also employed to $\psi_s^N (= n)$ and $\phi_s^K (= K^0)$.) The value of these couplings are given in Table 1. We do not present the explicit form of the potential here, because it is given in detail in ref [10].

The potential is given by the Fourier transformation of the product of the propagator and the vertices in the Breit-Fermi reduction. As the baryons and also the mesons have finite sizes and structures, we need to take a form factor at each meson-baryon vertex into account [22]. If we assume the same form factor $F(\mathbf{q}^2)$ for both the strong and weak vertices, the potential is given as

$$V(\mathbf{r}) = \int \frac{d^3q}{(2\pi)^3} \frac{e^{i\mathbf{q}\cdot\mathbf{r}}}{\mathbf{q}^2 + \mu^2 - q_0^2} \mathcal{O}(\mathbf{q}) F^2(\mathbf{q}^2) \quad (15)$$

where \mathcal{O} is a product of the vertex operators and the coupling constants. The operator \mathcal{O} includes the isospin operator,

$$\langle I | \boldsymbol{\tau}_1 \cdot \boldsymbol{\tau}_2 | I \rangle = \begin{cases} -3 & I = 0 \\ 1 & I = 1 \end{cases} .$$

In this case we use the initial state which is antisymmetrized in the flavor space.

A standard choice of $F^2(\mathbf{q}^2)$ is the square of the monopole form factor,

$$F_{DP}^2(\mathbf{q}^2) = \left(\frac{\Lambda_{DP}^2 - \mu^2}{\Lambda_{DP}^2 + \mathbf{q}^2} \right)^2 \quad (16)$$

which we call “double pole” (DP) form factor. While in literatures a simple form

$$F_{SP}^2(\mathbf{q}^2) = \frac{\Lambda_{SP}^2 - \mu^2}{\Lambda_{SP}^2 + \mathbf{q}^2} \quad (17)$$

is often used, which we call “single pole” (SP) form factor. The cutoff parameter Λ is chosen for individual mesons independently. These form factors are normalized at the on-mass-shell point as $F_{DP}^2(-\mu^2) = F_{SP}^2(-\mu^2) = 1$. There is another type of form factor, “Gaussian” (G),

$$F_G^2(\mathbf{q}^2) = \exp\left(-\frac{\mathbf{q}^2}{\Lambda^2}\right), \quad (18)$$

which has the advantage of the consistency with the quark structure for the baryon, if the cutoff parameter is taken according to the size of quark distribution in the baryon. This form factor is normalized as $F_G^2(0) = 1$. It should be noted that the SP and DP form factors give similar effects. Near at the mass shell point, F_{SP}^2 and F_{DP}^2 are expanded as

$$F^{SP} = \frac{\Lambda_{SP}^2 - \mu^2}{\Lambda_{SP}^2 + \mathbf{q}^2} = 1 - \left(\frac{\mathbf{q}^2 + \mu^2}{\Lambda_{SP}^2 + \mathbf{q}^2}\right) \quad (19)$$

$$F^{DP} = \left(\frac{\Lambda_{DP}^2 - \mu^2}{\Lambda_{DP}^2 + \mathbf{q}^2}\right)^2 \simeq 1 - 2\left(\frac{\mathbf{q}^2 + \mu^2}{\Lambda_{DP}^2 + \mathbf{q}^2}\right) \quad (20)$$

Therefore, the SP and DP form factors are identical if we set $\Lambda_{DP} \simeq \sqrt{2}\Lambda_{SP}$ by assuming $\Lambda^2 \gg \mu^2$. On the other hand, the G form factor behaves differently at short distances. Fig. 4 shows the behaviors of the potential for several form factors in the $\Lambda N : {}^3S_1 - NN : {}^3D_1$ OPE transition at the relative momentum of $k_r = 1.97\text{fm}^{-1}$. As can be seen clearly, the potential has a node for the G form factor, while the others do not behave like that. This oscillation suppresses the tensor transition although the long distance behavior is similar to the “hard” DP form factor or that without the form factor. We test these three form factors and compare the results.

We cannot neglect the finite energy transfer q_0 in eq. (15). In the case of typical nucleon-nucleon interaction, energy transfer is small and negligible, but in the case of $\Lambda N \rightarrow NN$ this energy transfer is not negligible because the mass-difference between Λ and N causes a large q_0 . If we assume that the initial $\Lambda - N$ pair has a low kinetic energy, this energy transfer is regarded as a constant, $q_0 \simeq (m_\Lambda - m_N)/2 \simeq 88\text{MeV}$. Accordingly we introduce effective masses of the exchanged mesons, $\tilde{\mu}_i = \sqrt{\mu_i^2 - (m_\Lambda - m_N)^2/4}$ and perform following replacement,

$$\frac{1}{\mathbf{q}^2 + \mu^2 - q_0^2} \rightarrow \frac{1}{\mathbf{q}^2 + \tilde{\mu}^2}. \quad (21)$$

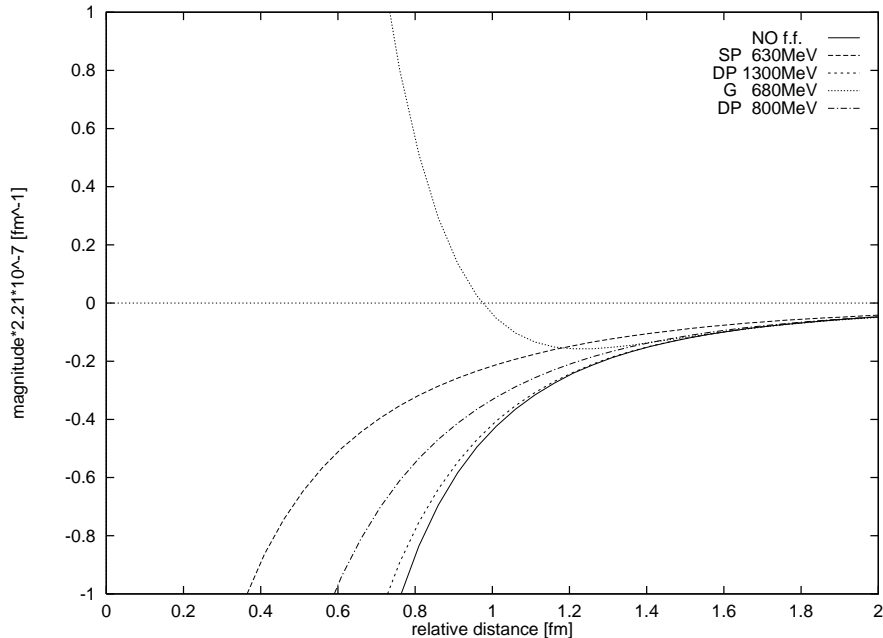


Figure 4: The OPE potentials for the ${}^3S_1 \rightarrow {}^3D_1$ for various form factors.

This effect leads to measurable changes. For example, the pion mass is reduced by about 25%, and the range of OPE becomes longer.

2.2 Direct Quark Mechanism

Studies of nuclear forces in the quark cluster model have revealed that the short range repulsion between nucleons is explained in terms of the quark exchange interactions [23]. The range of the strong repulsion is about 0.5 fm and corresponds to a momentum transfer of about 400 MeV/c. The same momentum transfer is required in the $\Lambda N \rightarrow NN$ transition in order to satisfy the energy-momentum conservation. It is therefore expected that the quark substructure of the baryons plays a significant role also in the short range part of the $\Lambda N \rightarrow NN$ interaction. Recently, we proposed the direct quark (DQ) mechanism, in which the weak interaction between quarks in baryons causes the decay without exchanging mesons Fig. 5 [13].

The weak interaction among constituent quarks is described as a $\Delta S = 1$ effective weak Hamiltonian, which consists of various four quark weak vertices derived in the renormalization group approach to include QCD corrections to the $su \rightarrow ud$ transition mediated by the W boson [24]. Such effective weak Hamiltonian has been applied to the decays of kaons and

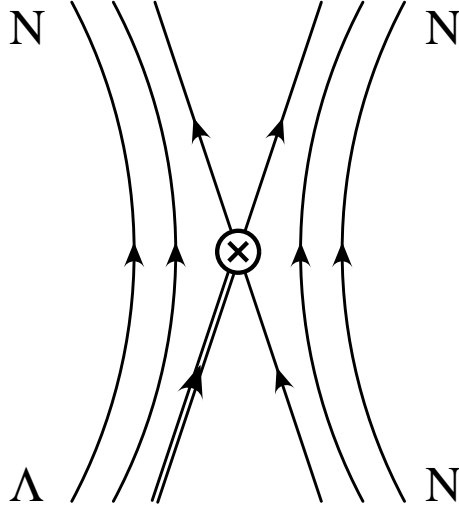


Figure 5: Direct quark mechanism for non-mesonic decay of hyperon. The double line indicates the strange quark, and \otimes stands for the weak vertex.

hyperons with considerable success. Our aim is to explain the short range part of the weak baryonic interaction by using the same interaction so that we are able to confirm the consistency between the free hyperon decays and decays of hypernuclei.

The transition potential is calculated by evaluating the effective Hamiltonian in the nonrelativistic valence quark model [13]. The valence quark wave function of two baryon system is taken from the quark cluster model, which takes into account the antisymmetrization among the quarks. Then the obtained transition potential has been applied to the weak decay of light hypernuclei [14].

In ref [13], the DQ transition potential is calculated for all the two-body channels with the initial $\Lambda N(L = 0)$ and the final $NN(L' = 0, 1)$ states. The explicit forms of the transition potential are given in the momentum space representation. In the present analysis, we employ the coordinate space formulation, so that realistic nuclear wave functions with short range correlations can be easily handled. The DQ transition potentials in the coordinate space contain nonlocal terms as a result of the quark antisymmetrization. It also has terms with a derivative operator acting on the initial relative coordinate. Thus the general form of the transition potential is

$$\begin{aligned}
 V_{DQ_{SS'J}}^{LL'}(r, r') &= \langle NN : L'S'J | V(\vec{r}', \vec{r}) | \Lambda N : LSJ \rangle \\
 &= V_{loc}(r) \frac{\delta(r - r')}{r^2} + V_{der}(r) \frac{\delta(r - r')}{r^2} \partial_r + V_{nonloc}(r, r')
 \end{aligned} \tag{22}$$

where r (r') denotes the relative radial coordinate of the initial (final) two-baryon state, and ∂_r stands for the derivative of the initial ΛN relative wave function. The explicit forms of $V_{loc}(r)$, $V_{der}(r)$, and $V_{nonloc}(r, r')$, are given in Appendix. It should be noted here that the DQ potential does not contain the tensor terms as we truncated the nonrelativistic expansion at the $O(p^2)$. We expect that the tensor component of the DQ transition is negligibly small.

Combining the direct quark (DQ) and meson exchange (ME) potentials, we obtain the total transition potential as

$$V(r, r') = V^{ME}(r) \frac{\delta(r - r')}{r^2} + V^{DQ}(r, r') \quad (23)$$

The relative phase between ME and DQ is fixed so that the weak quark Hamiltonian gives the correct amplitude of $\Lambda \rightarrow N\pi$ transition [14]. Note that the relative phases among various meson exchange potentials are determined according to the $SU(6)_w$ symmetry.

3 Nuclear Matter Calculation

Here we study the $\Lambda N \rightarrow NN$ decay in nuclear matter in order to investigate our approach to $\Lambda N \rightarrow NN$ with minimizing wave function model ambiguity. On top of that, the recent experimental data of life-times of heavy hypernuclei indicate that the nonmesonic decay rate of Λ in heavy hypernuclei is only about 20% larger than the free Λ decay rate [6]. This saturation suggests the short-range nature of the $\Lambda N \rightarrow NN$ decay. We study the Λ decay in nuclear matter as an approximation to the heavy Λ hypernuclei.

We assume that nuclear matter is symmetric ($N_n = N_p$) and the Λ is at rest in it. In this assumption the initial state density is given as

$$\int_0^{k_F} \frac{d^3k}{(2\pi)^3} \sum_{S_N} \times \frac{1}{2} \sum_{S_\Lambda} \times \sum_{p,n} \quad (24)$$

where S_N and S_Λ are the spin of nucleon and Λ hyperon respectively. Similarly, the final state density is

$$\int \frac{d^3k_1}{(2\pi)^3} \frac{d^3k_2}{(2\pi)^3} (2\pi)^4 \delta^4(E.M.C.) \sum_{S_{N_1} S_{N_2}} \quad (25)$$

where the $\delta(E.M.C)$ stands for the δ function coming from the energy momentum conservation. Then the $\Lambda N \rightarrow NN$ decay rate in symmetric nuclear matter becomes

$$\Gamma_{NM} = \int_0^{k_F} \frac{d^3k}{(2\pi)^3} \int \frac{d^3k_1}{(2\pi)^3} \int \frac{d^3k_2}{(2\pi)^3} (2\pi)^4 \delta^4(E.M.C.) \frac{1}{2} \sum_{spin} \sum_{p,n} | \langle \Psi_f(k_1, k_2) | V | \Psi_i(k, 0) \rangle |^2 \quad (26)$$

where $|\Psi_i(k, 0)\rangle$ stands for an initial ΛN state with the momentum of the nucleon k , and $|\Psi_f(k_1, k_2)\rangle$ stands for the final two nucleon state with the momenta k_1 and k_2 respectively. The V is $\Lambda N \rightarrow NN$ transition potential.

We employ the plane wave with the short range correlation for the wave function of both the initial and final states. The short range correlation represents the short range repulsion between two baryons. Therefore the configuration space wave function for the two baryon system with total momentum \mathbf{K} and relative momentum \mathbf{k} is

$$\langle \mathbf{R}, \mathbf{r} | \Psi(\mathbf{K}, \mathbf{k}) \rangle = \frac{1}{\sqrt{2}} e^{i\mathbf{K}\cdot\mathbf{R}} [e^{i\mathbf{k}\cdot\mathbf{r}} - (-1)^{S+I} e^{-i\mathbf{k}\cdot\mathbf{r}}] \chi_{Sm_S} \chi_{II_3} \times f(r) \quad (27)$$

where $f(r)$ is the correlation function and S and I are the spin and isospin of the two baryon system, respectively. We apply the correlation function proposed in ref [10]. For the initial ΛN , we employ

$$f_i(r) = \left(1 - e^{-\frac{r^2}{a^2}}\right)^n + br^2 e^{-\frac{r^2}{c^2}} \quad (28)$$

where $a = 0.5[\text{fm}]$, $b = 0.25[\text{fm}^{-2}]$, $c = 1.28[\text{fm}]$, $n = 2$, and for the final NN

$$f_f(r) = 1 - j_0(q_c r) \quad (29)$$

where $q_c = 3.93 \text{ fm}^{-1}$. The initial state correlation is obtained from a macroscopic finite nucleus G-matrix calculation, and the final state correlation gives a good description of nucleon pairs in ${}^4\text{He}$.

In the present calculation, we only consider the relative $L = 0$ for the initial $\Lambda - N$ system. Then the possible transition channels are those given in Table 2. The decay rate is decomposed as

$$\Gamma_{NM} = \Gamma_p + \Gamma_n \quad (30)$$

where the Γ_p and Γ_n stand for the proton- and neutron-induced decay rates respectively, and are given as

$$\Gamma_p = \frac{m_N}{(2\pi)^5 \mu^3} \int_0^{\mu k_F} k^2 k_0 dk \frac{1}{4} \left(|a_p|^2 + |b_p|^2 + 3|c_p|^2 + 3|d_p|^2 + 3|e_p|^2 + 3|f_p|^2 \right) \quad (31)$$

$$\Gamma_n = \frac{m_N}{(2\pi)^5 \mu^3} \int_0^{\mu k_F} k^2 k_0 dk \frac{1}{4} \left(|a_n|^2 + |b_n|^2 + 3|f_n|^2 \right) \quad (32)$$

$$k_0^2 \equiv m_N(m_\Lambda - m_N) + \frac{k^2}{2\mu} \quad (33)$$

$$\mu \equiv \frac{m_\Lambda}{m_N + m_\Lambda} \quad (34)$$

where the a, b, \dots, f are the matrix elements of the transition potential, for example,

$$a_p \equiv \langle {}^1S_0 : [pn]_{I=1} | V | {}^1S_0 : [\Lambda p]_s \rangle \quad (35)$$

3.1 Form Factor Dependence

As the $\Lambda N \rightarrow NN$ scattering involves a large momentum transfer, $\sqrt{m_N(m_\Lambda - m_N)c^2} \sim 400 \text{ MeV}/c$, the amplitudes are rather sensitive to the form factor. Here we show the dependence on form factor in meson exchange potential. First, we examine the form factor of OPE potential. Table 3 shows the calculated decay rate when we employ only OPE induced $\Lambda N \rightarrow NN$ potential. The SP form has often been used in literatures [3, 4]. McKeller and Gibson employed the SP form factor with $\Lambda_{SP}^2 = 20m_\pi^2$, or $\Lambda_{SP} \sim 630 \text{ MeV}$. This form factor is based on the dispersion relation analysis with the semi-pole approximation to the πNN form factor. It is a very soft form factor, which cuts off the short-range part rather drastically and the resulting decay rate becomes small. The tensor transition, $\Lambda p : {}^3S_1 \rightarrow pn : {}^3D_1$, is most affected by such form factor. We find that the tensor transition amplitudes are reduced by a factor two or more by the form factor. Therefore total decay rate much reduced as shown in Table 3

The DP form factor is popular in meson exchange potential models of the nuclear force. The Bonn potential [26], for instance, employs the DP with $\Lambda_{DP}(\pi) = 1300 \text{ MeV}$. This form factor is extremely hard so that the short range part of the meson exchange potential becomes relevant. The DP form factor is regarded as the product of the monopole form factors at the two πBB vertices. Lee and Matsuyama carried out an analysis of the $NN \rightarrow NN\pi$ processes and pointed out [27] that a soft form factor, such as $\Lambda < 750 \text{ MeV}$, is preferable. Recent analysis in the QCD sum rule also suggests a soft πNN form factor of cutoff $\Lambda \simeq 800 [\text{MeV}]$ [28]. From the quark substructure point of view, it is also natural that the cutoff Λ is of order $\sim 1/R_h \sim 400 - 500 \text{ MeV}$. Table 3 shows the comparison of the “hard” (DP, $\Lambda_{DP}(\pi) = 1300 \text{ MeV}$) and “soft” (DP, $\Lambda_{DP} = 800 \text{ MeV}$) pion-exchange form factors for the $\Lambda N \rightarrow NN$ decay rates. We find that the soft form factor reduces the decay rates by about 40%, while the hard one changes only by $\leq 10\%$.

The G form factor is related to the Gaussian quark wave function of the baryon. Corresponding to the size parameter $b \simeq 0.5 \text{ fm}$, we employ $\Lambda_G(\pi) \simeq 680 \text{ MeV}$ because the relation between the size and cutoff parameters is $\Lambda = \sqrt{3}/b$.

The above sensitivity to choice of the form factor is quite annoying because it is not easy to judge which of the form factors is the right one. It should also be noted that the weak

vertex form factor can be different from the strong one, although the pole dominance picture of the parity-conserving weak vertex leads to the identical form factor to the strong one. In the meson exchange potential models of the nuclear force, there seems a tendency to choose a hard form factor because the heavy meson exchanges are often important for spin-dependent forces. On the other hand, the quark model approach to the short range nuclear force gives significant spin dependencies comparable to the heavy meson exchanges and therefore the meson exchanges can be cut off rather sharply with a soft form factor. In the present approach to the weak $\Lambda N \rightarrow NN$ interaction, whose short range part is described by the direct quark mechanism, we thus may follow the quark model approach to the nuclear force and take the “soft” form factor for OPE potential as a standard. And we assume that the heavy meson (K , η , ρ , ω , K^*) exchanges have the similar DP form factors with the cutoff given by the Jülich potential [25]. We see that this choice gives the total decay rate of Λ in nuclear matter with the recent experimental data for heavy hypernuclear decays.

3.2 Decay Rates

The calculated decay rates of Λ in nuclear matter for several models are listed in Table 4. We show not only the results of soft DP form factor but also the result of hard DP form factor. The cutoff parameters for the soft DP form factor and the hard DP form factor are given in Table 3.

First of all, we can see that the OPE model predicts a large total decay rate in comparison with experiment for the heavy hypernuclei, even if we choose the softer cutoff. The tensor dominance property leads to the small Γ_n/Γ_p and PV/PC ratio.

One sees that the kaon exchange contribution reduces Γ_p by more than factor two. This mainly comes from the cancellation in the channel d_p . At same time, the kaon exchange contribution reduces Γ_n . Therefore, the n/p ratio remains small. The decay is dominated by the $J = 1$ channels.

When we include η , ρ , ω , and K^* (“all”) mesons, both the proton and neutron induced decays increase but the n/p ratio is still small ($\simeq 0.1$). It is interesting to see that the PV/PC ratio becomes large, when we include heavier mesons.

One sees in Table 4 that the magnitude of DQ itself is small compared to that of π or $\pi + K$. However, the DQ has a large Γ_n and a large n/p ratio. It is also shown that the DQ mechanism is dominated by the parity violating channels and thus produces a large PV/PC ratio. The characteristic behaviors of DQ will distinguish it from the other mechanisms.

Now we go to the results of our complete approach, i.e., meson exchange mechanism plus direct quark mechanism. One sees that the pion exchange contribution strongly depends on the choice of the form factor as stated before. The hard form factor does not suppress the potential

at short distances and yields a large OPE contribution. As we assume that the DQ has little contribution to the tensor channel, Γ_p is still too large in the case of $DQ + \pi$. Again, the K exchange reduces the tensor amplitude and thus Γ_p is suppressed by a factor 2. However Γ_n is reduced, at the same time, which results in the n/p ratio $\simeq 0.2$. This value seems too small compared to the experimental values for the medium and heavy hypernuclei.

Contribution beyond the π and K mesons does not improve the situation. It is also questionable whether the DQ mechanism and the vector meson exchanges are independent and can be superposed. The double counting problem for the vector mesons and DQ contribution in nuclear force is pointed out in ref [29]. We thus take the “ $DQ + \pi + K$ ” with the soft π form factor as our present best model for the nonmesonic Λ decay.

4 Light Hypernuclei

The same $\Lambda N \rightarrow NN$ transition potential is applied to the study of the nonmesonic weak decays of light s-shell hypernuclei, ${}^5_{\Lambda}He$, ${}^4_{\Lambda}He$, and ${}^4_{\Lambda}H$. We assume the harmonic oscillator shell model wave function for the initial nucleons, while the Λ single particle wave function calculated with a realistic Λ -nuclear potential, which has a repulsion at short distances. (See ref [14] for details.) We further consider the short-range correlation, which is multiplied to the relative two-body wave functions. We employ the same correlation functions as those used in the nuclear matter calculation.

The Gaussian b parameters are 1.358 [fm] for $A=5$ and 1.65 [fm] for $A=4$. For the final state, we assume the correlated plane waves for the outgoing two nucleons, and sum up all the residual states.

Here we present the results for the light hypernuclei and compare with the experimental one. Table 5 summarizes the results given by the superposition of the ME and DQ mechanism.

In this result we find that the “ $\pi + K + DQ$ ” picture gives us good agreement with experiment for the total decay rate, while the n/p ratios are still too small. As seen in the nuclear matter calculation, the main contribution comes from the OPE mechanism, which produces a large proton-induced rate. Comparing with the experimental data we find that the proton-induced rate is overestimated in all the pictures, while the neutron-induced rate is underestimated.

5 Summary and Conclusion

In this paper we study the $\Lambda N \rightarrow NN$ weak transition by combining the ME and DQ mechanisms. We use the weak meson-baryon coupling vertices which are evaluated by using $SU(6)_w$ symmetry. The DQ mechanism comes from the quark structure of two baryons and is effective at the short range where two baryons overlap with each other. Adding these two types of contributions, we calculate the decay rate of Λ in nuclear matter and in light hypernuclei. The choice of the form factor for the π exchange induced potential is found to be important. With the heavier mesons exchange or DQ for the short range part, it seems appropriate to employ the soft form factor for OPE.

In our calculation we find that the choice of “ $\pi + K + DQ$ ” with soft DP form factor for OPE reproduces the current experimental data rather well. The OPE contribution dominates the decay. The K contribution is also large and interferes destructively with the π contribution. These two contributions yield the long range part of this process. In the “ $\pi + K + DQ$ ” picture it is assumed that the DQ mechanism replaces the role of the heavier mesons.

Although the present analysis gives the total decay rates both in nuclear matter and in light hypernuclei fairly well, there remains a difficult problem. That is, the proton-induced decay rate is too large compared to experimental one and thus we predict a small n/p ratio. The ratio is improved from the $\pi + K$ exchange prediction due to the DQ contribution, in which the n/p ratio is about unity. It is, however, still small ($\simeq 0.2$) for “ $\pi + K + DQ$ ”. The experimental numbers are not completely fixed, but they suggest the value around 1 for heavy hypernuclei. The situation is similar for ${}^5_\Lambda\text{He}$. It is thus urgent and important to find out what causes this discrepancy.

Appendix

In this Appendix, we present the explicit forms of the DQ transition potential in the coordinate space. This is based on its momentum representation given in ref. [13] (referred to as (I) hereafter). The potential is expressed in terms of three sets of seven functions of k and k' , $f(k, k')_i$, $g(k, k')_i$, and $h(k, k')_i$, given in Tables 6, 7, and 8 of the paper (I). The complete transition potential is given by eq.(24) of the paper (I) as a combination of the functions, f , g , and h 's, and the coefficients, which depends on the initial and final orbital angular momenta, spins and isospin. Those coefficients denoted by V_i 's and W are explicitly given in Tables 2, 3, 4, and 5 in the paper (I), so that anyone can reconstruct the whole transition potential without any further information.

The purpose of this Appendix is to replace the functions, f , g , and h 's, by their Fourier

transformed counterparts, which are convenient for hypernuclear decays with sophisticated nuclear wave functions. In the coordinate space, the potential becomes nonlocal due to the quark antisymmetrization effect, and also contains a derivative term, which generates a transition from $L = 0$ to $L' = 1$. Such derivative terms appear for the functions, g and h 's. The complete potential is now given as a nonlocal form as

$$V_{DQSS'J}^{LL'}(r, r') = -\frac{G_F}{\sqrt{2}} \times W \sum_{i=1}^7 \left\{ V_i^f f_i(r, r') + V_i^g g_i(r, r') + V_i^h h_i(r, r') \right\} \quad (36)$$

where r (r') stands for the radial part of the relative coordinate in the initial (final) state. We only need to give the forms of the radial functions, f , g , and h 's as the coefficients, V_i 's and W , are the same ones as in the paper (I). (We, however, call the reader's attention that the transition potential given in the paper (I) is for the antisymmetrized initial states. They are antisymmetrized so that the flavor antisymmetric states are defined as $(p\Lambda - \Lambda p)/\sqrt{2}$ or $(n\Lambda - \Lambda n)/\sqrt{2}$. Thus they have an opposite sign to those commonly used in the literature for the meson exchange potential. It is necessary to take care of this difference in convention when we superpose the DQ potential with that from the meson exchange. If one adds our transition potential to the OPE in the conventional definition, we need to change the signs of the coefficients for the flavor-antisymmetric initial states.)

The local parts (with a derivative on the initial radial coordinate) are given for $i = 1, 6$, and 7, by

$$\begin{aligned} f_1(r, r') &= \frac{6}{N} 1 \cdot 1 \cdot (2\pi b^2)^{-3/2} \frac{\delta(r - r')}{r^2} \\ g_1(r, r') &= \frac{6}{N} 1 \cdot \frac{1}{\sqrt{3}m} \cdot (2\pi b^2)^{-3/2} (-i) \frac{\delta(r - r')}{r^2} \partial_r \\ h_1(r, r') &= \frac{6}{N} 1 \cdot \frac{1}{\sqrt{3}m} \cdot (2\pi b^2)^{-3/2} (-i) \frac{\delta(r - r')}{r^2} \partial_r \end{aligned} \quad (37)$$

$$\begin{aligned} f_6(r, r') &= \frac{9}{N} 1 \cdot 1 \cdot (4\pi A)^{-3/2} e^{-r^2/4A} \frac{\delta(r - r')}{r^2} \\ g_6(r, r') &= \frac{9}{N} 1 \cdot \frac{1}{\sqrt{3}m} \cdot (4\pi A)^{-3/2} e^{-r^2/4A} (-i) \frac{\delta(r - r')}{r^2} \partial_r \end{aligned} \quad (38)$$

$$\begin{aligned} h_6(r, r') &= \frac{9}{N} 1 \cdot \frac{1}{\sqrt{3}m} \cdot (4\pi A)^{-3/2} e^{-r^2/4A} (-i) \frac{\delta(r - r')}{r^2} \left[\partial_r + \frac{1}{2A} r \right] \\ f_7(r, r') &= -\frac{1}{3} f_6(r, r') \\ g_7(r, r') &= -\frac{1}{3} g_6(r, r') \end{aligned} \quad (39)$$

$$h_7(r, r') = -\frac{1}{3}h_6(r, r')$$

where $A \equiv b^2/3$, the normalization factor N is taken as $N = 1$ and ∂_r is the derivative on the initial radial coordinate.

Among the above local potentials, the f_1 part contains a constant term, which survives at $r = r' \rightarrow \infty$. This term comes from the internal weak conversion of Λ into a neutron and is to be suppressed due to the mismatch of the initial and final wave functions. However, in the application to hypernuclear decays we do not necessarily employ wave functions which satisfy the orthogonality condition of the bound and scattering states. Thus the f_1 term may survive in the actual calculation. As this term is spurious in most of the cases, we omit the f_1 term in the actual calculation.

The nonlocal parts are given in terms of the functions,

$$\begin{aligned} G_0 &\equiv (4\pi^2 D)^{-3/2} 4\pi i_0 \left(\frac{C r r'}{D} \right) \exp \left(\frac{-B' r'^2 - B r^2}{D} \right) \\ G_1 &\equiv (4\pi^2 D)^{-3/2} 4\pi i_1 \left(\frac{C r r'}{D} \right) \exp \left(\frac{-B' r'^2 - B r^2}{D} \right) \end{aligned} \quad (40)$$

where i_ℓ is the ℓ th modified spherical Bessel function.

For $i = 2$, the constants B , B' , C , and D are given by

$$B = B' = \frac{5b^2}{12} \quad C = \frac{b^2}{2} \quad D = \frac{4b^4}{9} \quad (41)$$

and we find

$$\begin{aligned} f_2(r, r') &= -\frac{18}{N} \frac{1}{3} \cdot 1 \cdot \frac{3\sqrt{6}}{4} G_0 \\ g_2(r, r') &= -\frac{18}{N} \frac{1}{3} \cdot \frac{1}{\sqrt{3}m} \cdot \frac{3\sqrt{6}}{4} (i) \left[-\frac{2B}{D} r G_1 + \frac{C}{D} r' G_0 \right] \\ h_2(r, r') &= -\frac{18}{N} \frac{1}{3} \cdot \frac{1}{\sqrt{3}m} \cdot \frac{3\sqrt{6}}{4} (-i) \left[-\frac{2B'}{D} r' G_0 + \frac{C}{D} r G_1 \right] \end{aligned} \quad (42)$$

For $i = 4$,

$$f_4(r, r') = -\frac{36}{N} \frac{1}{3} \cdot 1 \cdot \frac{3\sqrt{3}}{8} G_0$$

$$\begin{aligned}
g_4(r, r') &= -\frac{36}{N} \frac{1}{3} \cdot \frac{1}{\sqrt{3}m} \cdot \frac{3\sqrt{3}}{8} (i) \left[-\frac{2B}{D} rG_1 + \frac{C}{D} r'G_0 \right] \\
h_4(r, r') &= -\frac{36}{N} \frac{1}{3} \cdot \frac{1}{\sqrt{3}m} \cdot \frac{3\sqrt{3}}{8} (-i) \left[-\frac{2B'}{D} r'G_0 + \frac{C}{D} rG_1 \right]
\end{aligned} \tag{43}$$

with

$$B = B' = \frac{b^2}{6} \quad C = 0 \quad D = \frac{b^4}{9} \tag{44}$$

For $i = 3$, and $i = 5$, we find

$$\begin{aligned}
f_3(r, r') &= -\frac{36}{N} \frac{1}{3} \cdot 1 \cdot \frac{24\sqrt{33}}{121} G_0 \\
g_3(r, r') &= -\frac{36}{N} \frac{1}{3} \cdot \frac{1}{\sqrt{3}m} \cdot \frac{24\sqrt{33}}{121} (i) \left[-\frac{2B}{D} rG_1 + \frac{C}{D} r'G_0 \right] \\
h_3(r, r') &= -\frac{36}{N} \frac{1}{3} \cdot \frac{1}{\sqrt{3}m} \cdot \frac{24\sqrt{33}}{121} (-i) \left[-\frac{2B'}{D} r'G_0 + \frac{C}{D} rG_1 \right]
\end{aligned} \tag{45}$$

with for $i = 3$,

$$B = \frac{13b^2}{33} \quad B' = \frac{7b^2}{33} \quad C = \frac{12b^2}{33} \quad D = \frac{20b^4}{99} \tag{46}$$

and for $i = 5$,

$$B = \frac{7b^2}{33} \quad B' = \frac{13b^2}{33} \quad C = \frac{12b^2}{33} \quad D = \frac{20b^4}{99} \tag{47}$$

The local parts of the DQ, π -, K - exchange potentials are illustrated in Fig. 6 for the proton induced transitions and Fig. 7 for the neutron induced one. The meson exchange potentials are multiplied by the form factors. We take the soft ($\Lambda_\pi = 800\text{MeV}$) DP form factor for OPE.

References

- [1] J. F. Donoghue, E. Golowich, and B. Holstein, Phys. Rep. **131** 319 (1986).
- [2] M. M. Block, and R. H. Dalitz, Phys. Rev. Lett. **11** 96 (1963).
- [3] B. H. J. McKeller, and B. F. Gibson, Phys. Rev. **C30**, 322 (1984).
- [4] K. Takeuchi, H. Takaki, and H. Bando, Prog. Theor. Phys. **73** 841 (1985); H. Bando, Y. Shono, and H. Takaki, Int. Jour. Mod. Phys. **A3** 1581 (1988).
- [5] E. Oset and L. L. Salcedo, Nucl. Phys. **A443** 704 (1985); A. Ramos, E. Oset, and L. L. Salcedo, Phys. Rev. **C50** 2314 (1994).
- [6] H. Bando, T. Motoba, and J. Zofka, Int. Jour. Mod. Phys. **A5** 4021 (1990).
- [7] A. Ramos, E. van Meijgaard, C. Bennhold, and B. K. Jennings, Nucl. Phys. **A544** 703 (1992).
- [8] A. Parreño, A. Ramos, and E. Oset, Phys. Rev. **C51**, 2479 (1995); A. Parreño, A. Ramos, and C. Bennhold, Phys. Rev. **C52**, R1768 (1995).
- [9] J. F. Dubach, G. B. Feldman, B. R. Holstein, and L. de la Torre, Ann. Phys. **249**, 146 (1996).
- [10] A. Parreño, A. Ramos, and C. Bennhold, Phys. Rev. **C56**, 339 (1997).
- [11] C. H. Cheung, D. P. Heddle, and L. S. Kisslinger, Phys. Rev. **C27** 335 (1983).
- [12] K. Maltman and M. Shmatikov, Phys. Lett. **B331** 1(1994).
- [13] T. Inoue, S. Takeuchi, and M. Oka, Nucl. Phys. **A577** 281c (1994); *ibid* **A597** 563 (1996).
- [14] T. Inoue, M. Oka, T. Motoba, and K. Itonaga, Nucl. Phys. **A633** 312 (1998).
- [15] M. Shmatikov, Nucl. Phys. **A580** 538 (1994).
- [16] K. Itonaga, T. Ueda, and T. Motoba, Nucl. Phys. **A639** 329c (1998).
- [17] J. J. Szymanski et al., Phys. Rev. **C43** 849 (1991).
- [18] H. Noumi et al., Phys. Rev. **C52** 2936 (1995).

- [19] H. Bhang et al., Phys. Rev. Lett. **81** 4321 (1998).
- [20] H. Noumi et al., in proceedings of the IV International Symposium on Weak and Electromagnetic Interactions in Nuclei, edited by H. Ejiri, T. Kishimoto and T. Sato (World Scientific, 1995) p.550
- [21] M. N. Nagels, T. A. Rijken, and J. J. Swart, Phys. Rev. D**15**, 2547 (1977); P. M. M. Maessen, T. A. Rijken, and J. J. de Swart, Phys. Rev. C**40**, 2226 (1989).
- [22] V. G. J. Stoks, R. A. M. Klomp, C. P. F. Terheggen, and J. J. de Swart, Phys. Rev. C**49** 2950 (1994).
- [23] M. Oka and K. Yazaki, Phys. Lett. B**90** 41 (1980); Prog. Theor. Phys. **66** 556 (1981) *ibid* **66** 572 (1981); in *Quarks and Nuclei*, ed. by W. Weise (World Scientific, 1985); K. Shimizu, Rep. Prog. Phys. **52** 1 (1989).
- [24] M. K. Gaillard and B. W. Lee, Phys. Rev. Lett. **33** 108 (1974); A. I. Vainshtein, V. I. Zakharov and M. A. Shifman, Sov. Phys. JETP **45** 670 (1977); F. J. Gillman, M. B. Wise, Phys. Rev. D**20** 2382 (1979); E. A. Paschos, T. Schneider and Y. L. Wu, Nucl. Phys. B**332** 285 (1990).
- [25] B. Holzenkamp, K. Holinde, and J. Speth, Nucl. Phys. A**500** 485 (1989).
- [26] R. Machleidt, K. Holinde, and Ch. Elster, Phys. Rep. **149**, 1 (1987)
- [27] T. S. H. Lee and A. Matsuyama, Phys. Rev. C**36** 1459 (1987).
- [28] T. Meissner, Phys. Rev. C**52** 3386 (1995).
- [29] K. Yazaki, Prog. Part. Nucl. Phys. **24** 353 (1990).

Table 1: The strong and weak meson baryon coupling constants. The strong coupling constants are taken according to the Nijmegen potential (soft core) [21]. The weak coupling constants are estimated by ref [10]. They are in units of $G_F m_\pi^2 = 2.21 \times 10^{-7}$. The cutoff parameters for the DP form factor are also given.

Meson	Strong c.c.	Weak c.c.		Λ [MeV]	
		PC	PV	soft	hard
π	$g_{NN\pi} = 13.3$ $g_{\Lambda\Sigma\pi} = 12.0$	$B_\pi = -7.15$	$A_\pi = 1.05$	800	1300
η	$g_{NN\eta} = 6.40$ $g_{\Lambda\Lambda\eta} = -6.56$	$B_\eta = -14.3$	$A_\eta = 1.80$	1300	1300
K	$g_{\Lambda NK} = -14.1$ $g_{N\Sigma K} = 4.28$	$C_K^{PC} = -18.9$ $D_K^{PC} = 6.63$	$C_K^{PV} = 0.76$ $D_K^{PV} = 2.09$	1200	1200
ρ	$g_{NN\rho}^V = 3.16$ $g_{NN\rho}^T = 13.1$ $g_{\Lambda\Sigma\rho}^V = 0$ $g_{\Lambda\Sigma\rho}^T = 11.2$	$\alpha_\rho = -3.50$ $\beta_\rho = -6.11$	$\epsilon_\rho = 1.09$	1400	1400
ω	$g_{NN\omega}^V = 10.5$ $g_{NN\omega}^T = 3.22$ $g_{\Lambda\Lambda\omega}^V = 7.11$ $g_{\Lambda\Lambda\omega}^T = -4.04$	$\alpha_\omega = -3.69$ $\beta_\omega = -8.04$	$\epsilon_\omega = -1.33$	1500	1500
K^*	$g_{\Lambda NK^*}^V = -5.47$ $g_{\Lambda NK^*}^T = -11.9$ $g_{N\Sigma K^*}^V = -3.16$ $g_{N\Sigma K^*}^V = -3.16$	$C_{K^*}^{PC,V} = -3.61$ $C_{K^*}^{PC,T} = -17.9$ $D_{K^*}^{PC,V} = -4.89$ $D_{K^*}^{PC,T} = 9.30$	$C_{K^*}^{PV} = -4.48$ $D_{K^*}^{PV} = 0.60$	2200	2200

Table 2: Possible ${}^{2S+1}L_J$ channels for the $\Lambda N \rightarrow NN$ transitions. I_f stands for the total isospin of the final state. PC and PV indicate the parity conserving and parity violating channels respectively.

1S_0	\rightarrow	1S_0	:	$I_f = 1$	a_p	a_n	:	PC
1S_0	\rightarrow	3P_0	:	$I_f = 1$	b_p	b_n	:	PV
3S_1	\rightarrow	3S_1	:	$I_f = 0$	c_p		:	PC
3S_1	\rightarrow	3D_1	:	$I_f = 0$	d_p		:	PC
3S_1	\rightarrow	1P_1	:	$I_f = 0$	e_p		:	PV
3S_1	\rightarrow	3P_1	:	$I_f = 1$	f_p	f_n	:	PV

Table 3: Decay rates of Λ in nuclear matter (in units of $\Gamma_\Lambda = (263 \times 10^{-12} \text{sec})^{-1}$) for various choices of the coupling form factors in the OPE mechanism.

		<i>total</i>	Γ_p	Γ_n	Γ_n/Γ_p	<i>PV/PC</i>
π	no-f.f.	2.819	2.571	0.248	0.097	0.358
	SP $\Lambda_\pi = 630\text{MeV}$	1.103	0.989	0.114	0.116	0.408
	$\Lambda_\pi = 920\text{MeV}$	2.332	2.116	0.216	0.102	0.376
	DP $\Lambda_\pi = 1300\text{MeV}$	2.575	2.354	0.221	0.094	0.337
	$\Lambda_\pi = 800\text{MeV}$	1.850	1.702	0.148	0.087	0.282
	G $\Lambda_\pi = 680\text{MeV}$	1.514	1.129	0.386	0.342	0.580

Table 4: Nonmesonic decay rates of Λ in nuclear matter (in units of Γ_Λ). The “all” includes π , K , η , ρ , ω , and K^* meson exchanges. Some recent experimental data for medium-heavy hypernuclei are also given.

		<i>total</i>	Γ_p	Γ_n	Γ_n/Γ_p	<i>PV/PC</i>
π	DP hard	2.575	2.354	0.221	0.094	0.337
	DP soft	1.850	1.702	0.148	0.087	0.282
	no-f.f.	2.819	2.571	0.248	0.097	0.358
$\pi+K$	DP hard	1.099	1.075	0.024	0.022	0.631
	DP soft	0.695	0.674	0.021	0.031	0.632
	no-f.f.	1.143	1.111	0.032	0.028	0.745
all	DP hard	1.672	1.571	0.101	0.064	1.468
	DP soft	1.270	1.152	0.117	0.101	1.537
	no-f.f.	1.744	1.704	0.040	0.024	2.952
DQ		0.418	0.202	0.216	1.071	6.759
DQ+ π	DP hard	3.609	2.950	0.658	0.223	0.856
	DP soft	2.726	2.202	0.523	0.238	0.896
DQ+ $\pi+K$	DP hard	1.766	1.495	0.271	0.181	1.602
	DP soft	1.204	0.998	0.206	0.207	1.954
DQ+all	DP hard	3.591	3.019	0.572	0.189	3.188
	DP soft	1.884	1.522	0.361	0.237	3.587
$\Gamma_\Lambda^{(12C)}$	EXP [17]	1.14 ± 0.2	—	—	$1.33_{-0.81}^{+1.12}$	—
$\Gamma_\Lambda^{(12C)}$	EXP [18]	$0.89 \pm 0.15 \pm 0.03$	$0.31_{-0.11}^{+0.18}$	—	$1.87 \pm 0.59_{-1.00}^{+0.32}$	—
$\Gamma_\Lambda^{(12C)}$	EXP [19]	1.14 ± 0.08	—	—	—	—
$\Gamma_\Lambda^{(28Si)}$	EXP [19]	1.28 ± 0.08	—	—	—	—
$\Gamma_\Lambda(Fe)$	EXP [19]	1.22 ± 0.08	—	—	—	—

Table 5: Nonmesonic decay rates (in units of Γ_Λ) of light hypernuclei. The DP (soft) form factor is used for OPE.

	<i>total</i>	Γ_p	Γ_n	Γ_n/Γ_p	
${}^5_\Lambda He$	π	0.740	0.654	0.087	0.133
	$\pi + K$	0.350	0.331	0.028	0.055
	$\pi + K + DQ$	0.521	0.435	0.085	0.195
	EXP [17]	0.41 ± 0.14	0.21 ± 0.07	0.20 ± 0.11	0.93 ± 0.55
	EXP [20]	0.50 ± 0.07	0.17 ± 0.04	0.33 ± 0.04	1.97 ± 0.67
${}^4_\Lambda He$	π	0.542	0.498	0.044	0.089
	$\pi + K$	0.252	0.233	0.019	0.082
	$\pi + K + DQ$	0.309	0.302	0.007	0.024
	EXP [20]	0.19 ± 0.04	0.15 ± 0.02	0.04 ± 0.02	0.27 ± 0.14
${}^4_\Lambda H$	π	0.080	0.022	0.056	2.596
	$\pi + K$	0.020	0.010	0.010	1.099
	$\pi + K + DQ$	0.120	0.060	0.059	0.983
	EXP [20]	0.15 ± 0.13	—	—	—

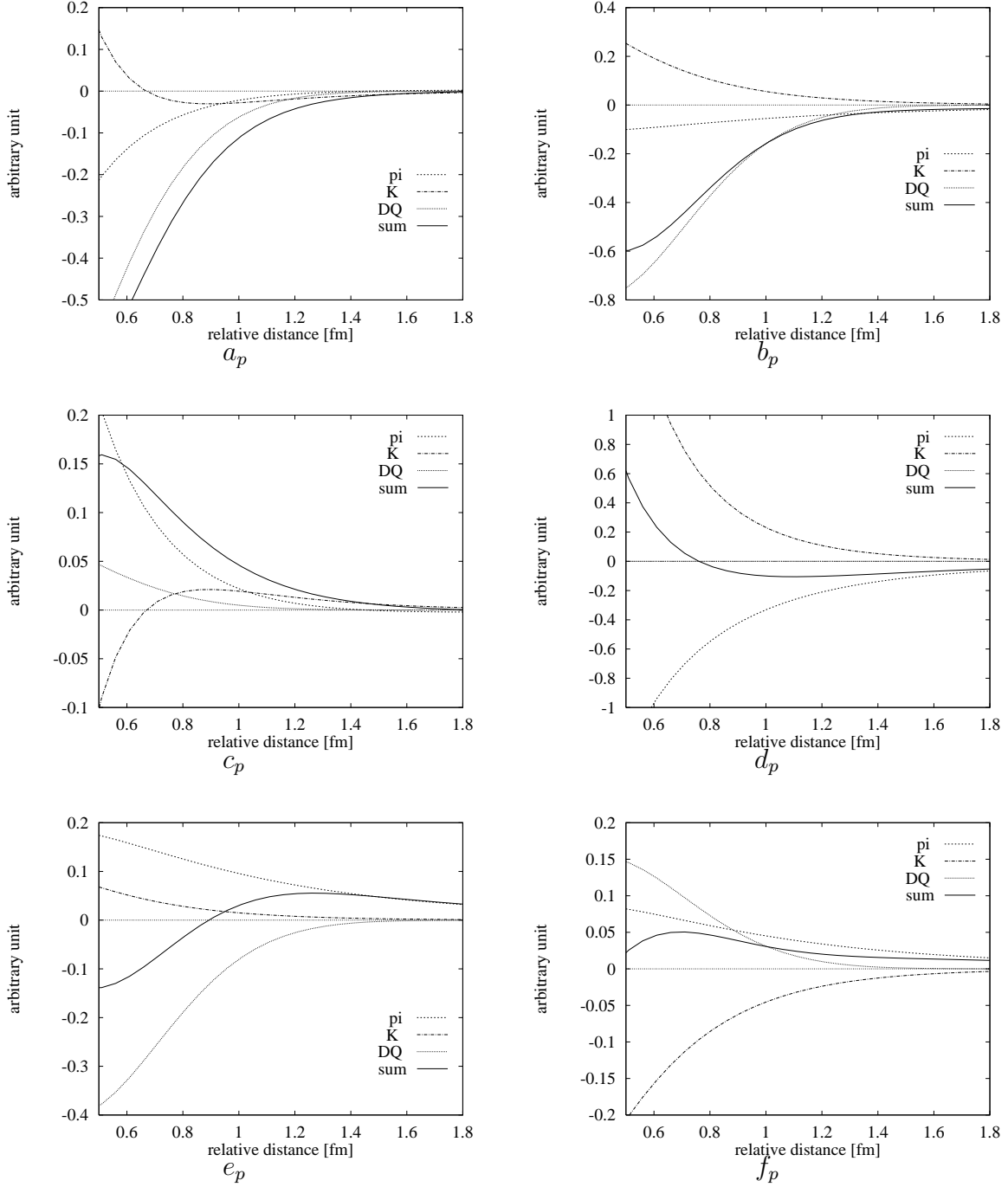


Figure 6: The transition potentials for the proton-induced decay.

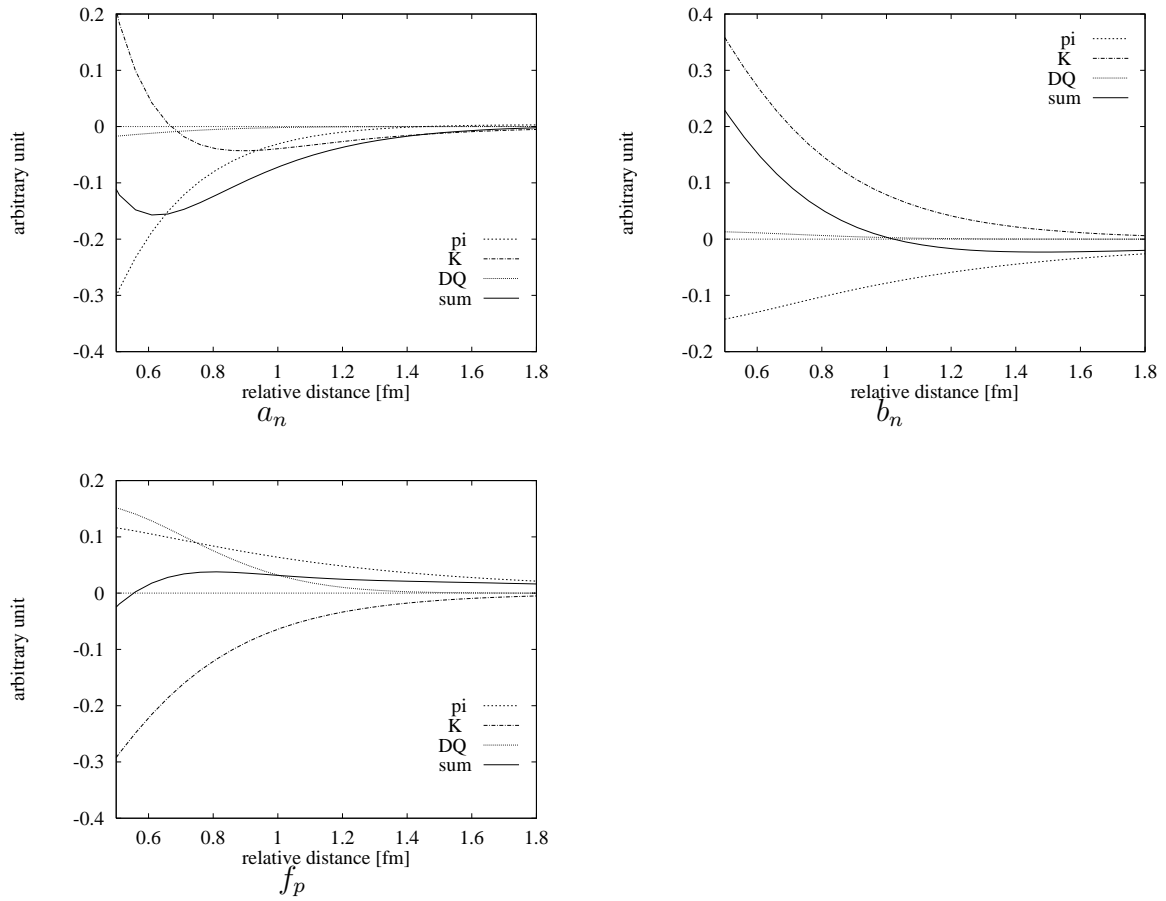


Figure 7: The transition potentials for the neutron-induced decay.